Accepted Manuscript

Title: Sustainable degradation of carbon tetrafluoride to non-corrosive useful products by incorporating reduced electron mediator within electro-scrubbing

Authors: G. Muthuraman, A.G. Ramu, Y.H. Cho, E.J. McAdam, I.S. Moon

Please cite this article as: G.Muthuraman, A.G.Ramu, Y.H.Cho, E.J.McAdam, I.S.Moon, Sustainable degradation of carbon tetrafluoride to non-corrosive useful products by incorporating reduced electron mediator within electro-scrubbing, Journal of Industrial and Engineering Chemistry https://doi.org/10.1016/j.jiec.2018.02.025

Sustainable degradation of carbon tetrafluoride to non-corrosive useful products by incorporating reduced electron mediator within electro-scrubbing

G. Muthuraman[a], A.G. Ramu[a], Y. H. Cho[b], E.J. McAdam[c], and I. S. Moon[a]*
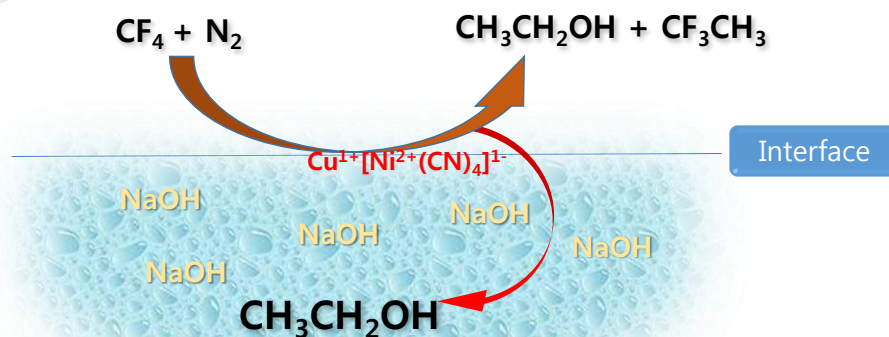
[a]Department of Chemical Engineering, Sunchon National University, #255 Jungangno, Suncheon 540-742, Jeollanam-do, Rep. of Korea.

[b]Korea Atomic Energy Research Institute, Yuseong P.O Box 105, Daejeon, Rep. of Korea

[c]Cranfield Water Science Institute, Cranfield University, Building 39, MK43 0AL, UK

*Corresponding Author: Tel: +82 61 750 3581; Fax: +82 61 750 3581
E-mail: ismoon@sunchon.ac.kr

Graphical Abstract

$$CF_4 + N_2 \qquad\qquad CH_3CH_2OH + CF_3CH_3$$

$$Cu^{1+}[Ni^{2+}(CN)_4]^{1-}$$

Interface

NaOH   NaOH   NaOH   NaOH   NaOH

$$CH_3CH_2OH$$

Synopsis: Ethanol generation was established during the degradation of CF_4 by mediated electrocatalytic reduction using electrogenerated $Cu^{1+}[Ni^{2+}(CN)_4]^{1-}$ at electro-scrubbing process.

Highlights

- A $Cu^{2+}[Ni^{2+}(CN)_4]$ complex was established for carbon tetrachloride degradation to non-corrosive useful product

- ORP and ESR results demonstrated Cu^{1+} formation at cathodic half-cell during electrolysis

- Mass transfer analysis identifies rate limiting behavior and routes to optimization

- Ethanol found to be a main product in the degradation of CF_4 my MER at electro-scrubbing

Abstract

The degradation of CF_4 gas using existing technologies produces other types of greenhouse gas (CO_2) and corrosive side products. The main aim of this study is to degrade CF_4 gas at room temperature into useful products without producing corrosive side products by mediated electrochemical reduction (MER) process using an electrogenerated $Cu^{1+}[Ni^{2+}(CN)_4]^{1-}$ mediator. Initial studies on the electrolytic reduction of the hetero-bimetallic complex in catholyte solution at anodized Ti cathode was monitored by oxidation/reduction potential (ORP) variation whether the Cu^{2+} or Ni^{2+} was reduced in the $Cu^{2+}[Ni^{2+}(CN)_4]$ and confirmed by electron spin resonance (ESR) spectroscopy the $Cu^{1+}[Ni^{2+}(CN)_4]^{1-}$ formation. The concentration variation of $Cu^{1+}[Ni^{2+}(CN)_4]^{1-}$ during CF_4 injection demonstrated the

degradation of CF_4 followed the MER by electrogenerated $Cu^{1+}[Ni^{2+}(CN)_4]^{1-}$. Maximum removal efficiency of CF_4 using electroscrubbing process was 96% at room temperature. Through the variation in gas phase parameters, the gas phase mass transfer coefficient was calculated that can facilitate scale up the developed process. Fourier transform infrared spectroscopy analysis in both the gas and solution phases showed that CH_3CH_2OH was the main product that formed during the removal of CF_4 by electrogenerated $Cu^{1+}[Ni^{2+}(CN)_4]^{1-}$ at electroscrubber along with a small amount of CF_3CH_3 intermediate. Importantly, this mechanism also avoided formation of the corrosive product HF.

1. Introduction

Both etching and cleaning steps in semiconductor manufacturing make use of perfluoro gases, such as CF_4, NF_3 and SF_6, which possess high global warming potential (GWP) [1]. Consequently, growth in electronic equipment demand is driving considerable increase in GWP through the fugitive release of perfluo gases into the environment. Of particular concern is CF_4 which has 6500 time GWP of CO_2 [2]. However, there are currently only a limited number of abatement technologies for perfluoro gases, which constitutes an extremely challenging separation. The two primary existing technologies are combustion and plasma arc [3-6]. Whilst the plasma etching technique could potentially be used in the electronic manufacturing industries, plasma will not typically achieve complete perfluoro gas degradation which results in formation of byproducts, notably another greenhouse gas, CO_2, and its derivatives (COF_2, CO, H_2O), with HF depending on the carrier gas [7-10]. Catalytic

combustion has also attracted considerable interest [11,12], particularly hydrolytic combustion because of its lower Gibbs free energy (-150 kJ/mol). Unfortunately, one of the final products obtained is highly corrosive HF, as shown in reaction 1, which leads to catalyst deactivation [13]. Also, another product in the catalytic combustion in the CF_4 decomposition process is CO_2, thereby further exacerbating greenhouse gas production.

$$CF_4 + 2H_2O \longrightarrow CO_2 + 4HF \,(\Delta G = -\,150 \text{ kJ/mol}) \,[11,12] \quad\quad \text{--- (1)}$$

The degradation of chloro fluoro carbons (CFCs) to mostly non-fluoro compounds has been achieved by electrochemical technique at room temperature without producing final products that contribute to greenhouse effects [14-16]. Copper supported gas diffusion electrode resulted in methane in degradation of $CClF_3$(CFC-13), and on Ag-supported gas diffusion electrode to form CHF_3 [14]. The degradation of many CFCs have been performed in solution phase especially through direct electrochemical reduction on different metal electrodes in acetonitrile [17] and DMF [18] to produce, CF_2CF_2, CH_2F_2, CH_3F, CF_2CFCl, and $CHCF_3$, as the main products, which are used as raw materials in the production of polymers and refrigerants. A methanol/water solvent mixture was also demonstrated to degrade CFC-11 and CFC-113 using a Pb cathode with a Pd containing gas diffusion anode by constant potential electrolysis, where complete or partially dehalogenated products were achieved depending on the Pd contents [19]. To improve understanding, fundamental electrochemical studies were performed on selective site-specific PFC compounds, which showed that the reduction reaction follows a radical reaction with the formation of a carbanion with subsequent oligomeric products, such as C_3H_8, C_3F_8, and CH_4 from CF_4 etc [20]. Most electrochemical studies on CFC degradation were performed in non-aqueous media or a combination of non-aqueous and aqueous solvents using electrochemical analyzer such as CV or constant potential electrolysis;

none were performed in only aqueous medium and a constant current electrolysis in the CFCs or CF_4 degradation process. Recently, CF_4 removal was reported using a mediated electrochemical reduction (MER) in aqueous KOH medium at room temperature by the electrochemically generated mediator Co^{1+} in an electro-scrubbing process [21]. Though, the main focus was development of room temperature removal of CF_4 by electroscrubbing (for the first time), the product found in the Co^{1+} MER of CF_4 were HF and ethanol [21]. The HF formation not only constitutes an environmental concern but may also reduce the pH of the electrolyte in continuous electro-scrubbing process, which will inactivate mediator generation, subsequently limiting CF_4 removal. Consequently, provided HF formation can be avoided, sustained CF_4 degradation could be achieved, coupled with the generation of ethanol that could be conceived as a sustainable high-value end product. One alternative could be utilization of a binary metal complex or bimetallic complex in the CF_4 degradation process. Note that to minimize catalyst deactivation in catalytic combustion process, a binary metal catalyst was attempted to degrade CF_4 by hydrolytic combustion process, with the idea of C-F bond breaking at the Lewis-acid catalysts to form metal fluorides, which was hydrolyzed, and made possible the assessment of various bimetal combinations. The study found that Ga-Al and Ni-Al oxide catalysts were stable from HF deactivation [22-24]. In another study, the CF_4 was converted to CO_2 with minimal deactivation (by HF formation) of the γ-Al_2O_3 catalysts by the addition of Zn, Ni, Mg, Sr, and Ba metals [7]. A stable catalyst was achieved in catalyst combustion process using Ce/Al_2O_3 binary catalyst but that was not effective in the removal of CF_4 [24].

In the present investigation, it is asserted that the hetero-bimetallic complex $Cu^{2+}[Ni^{2+}(CN)_4]$ can be used as a mediator precursor in the degradation of CF_4 gas to form a

useful end product and without the production of harmful sideproducts like HF . A constant current method was used to generate low valent active mediator generation in 10 M KOH medium at cathodic half-cell in a divided electrolytic cell to generate a low valent active mediator. An anodized Ti or TiO$_2$ cathode was used for the electrolytic reduction of Cu^{2+}[Ni^{2+}(CN)$_4$] in 10 M KOH. The oxidation/reduction potential (ORP) of Cu^{2+} and Ni^{2+} in a dissolved electrolyzed solution during electrolysis were taken as an indication and quantification by a potentiometric titration separately for the formation of a low oxidation state active mediator. In addition, electron spin resonance (ESR) spectroscopy was used to support the differentiation of Cu^{2+} or Ni^{2+} reduction in an electrolyzed solution. CF$_4$ degradation was carried out within an electro-scrubber, where CF$_4$ was fed continuously at a controlled rate and concentration through the bottom of the scrubber and the spent hetero-bimetallic complex was then sent to a cathodic half-cell to generate a low oxidation state active mediator. The CF$_4$ removal efficiencies were monitored using online Fourier transform infrared (FTIR). Solution phase and gas phase analyses were conducted to determine the final product.

2. Materials and Methods

2.1 Preparation of mediator precursor.

The hetero-bimetallic Cu^{2+}[Ni^{2+}(CN)$_4$] was prepared using the literature procedure [25]. In brief, Cu^{2+}(NO$_3$)$_2$.3H$_2$O and [Ni^{2+}(CN)$_4$]$^{2-}$ were added to 200 ml of water at a Cu^{2+} to Ni^{2+} mole ratio of 1:4. A light blue precipitate formed slowly with constant stirring, which was separated by filtration, washed several times with water and dried in a desiccator prior to use. [Ni^{2+}(CN)$_4$]$^{2-}$ was prepared using the existing literature procedure [26]. Briefly, Ni^{2+}(NO$_3$)$_2$.6H$_2$O was taken at a 1:4 mole ratio (Ni^{2+} to cyanide) to KCN, which was already

dissolved in 200 ml cooled water (extreme care was taken when handling the KCN during complex preparation because it is highly dangerous to humans). To this reaction solution, an equal volume of chilled alcohol was then added. The resulting thin orange platelets were filtered rapidly, washed with cold alcohol, recrystallized in ethanol, dried in a vacuum desiccator, and stored in an air-tight brown bottle.

2.2 Setup and procedure for mediator generation and degradation.

A divided flow-through electrolytic cell was used, as in a previous publication [21], under suitable additional conditions (Fig.1). Briefly, a 4 cm^2 working electrode area capacity thin layer plate and frame divided cell (divided with Nafion324) was connected to the catholyte (200 ml of mediator precursor in 10 M KOH) and anolyte (200 ml of 5 M H_2SO_4) glass tanks through polycarbon tubing to allow the anolyte and catholyte to circulate (using peristaltic pumps) through the respective anode and cathode compartments. The electrolysis experiments were conducted in constant current mode using a DC power supply. All solutions were prepared using reverse osmosis purified water (Human Power III plus, South Korea) with a resistivity of 18 MΩ-cm.

For the electro-scrubbing process, a 50 cm^2 electrode area capacity divided plate and frame electrochemical cell was connected to a 40 cm high and 5.5 cm (i.d) column packed with 1 cm^2 of Teflon tubes as the packing material on top of the catholyte tank (1 L capacity), as in Fig.1 and the previous published literature [21]. The electrolyte solutions (500 ml) were circulated continuously to flow through the electrolytic cell at different flow rates (1 to 5 L min^{-1}) using magnetic pumps. The catholyte solution as a scrubbing solution (electrolyzed mediator in a KOH solution) was pumped separately into the scrubber column at a flow rate of 3 L min^{-1}. CF_4 gas (from RIGAS (1000 ppm), Korea) and N_2 mixtures, which were obtained by the

controlled mixing of air and CF_4 gas using mass flow controllers (MFCs), were introduced to the bottom of the scrubber at a set gas flow rate. An online gas analyzer (FTIR) was attached to the scrubber exit to facilitate the instantaneous degradation measurements. Before each electrolysis experiment, the Ti electrode (cathode) was pretreated separately by an anodization process in 0.1 M KNO_3 at a constant current of 1 A for 5 min. All experiments were conducted at room temperature (20 ± 2 ºC).

2.3 Quantification of mediator ion.

The electrolyzed solution containing the Cu^{1+} or Ni^{1+} concentrations were determined using a potentiometric titration method [21]. In the present case, the electrolyzed sample solution was titrated against a standard $Fe^{3+}(CN)_6{}^{3-}$ (From Sigma Aldrich, USA) solution (0.001 M) and the potential variation was monitored using an ORP (oxidation/reduction potential) electrode (EMC 133, 6 mm Pt sensor electrode and Ag/AgCl reference electrode containing a gel electrolyte) connected to an iSTEK multimeter. The initial catholyte $(Cu^{2+}[Ni^{2+}(CN)_4])$ solution potential was approximately -170 mV, which was then decreased as electrolysis progressed at a constant current density. By titration against 0.001 M $[Fe^{3+}(CN)_6]^{3-}$, the initial ORP value showed that the Fe^{3+} concentration can be used to derive the concentration of Cu^{1+}.

2.4 Analysis.

Gas phase online analysis was performed using an online FTIR gas analyzer (from MIDAC Corporation, USA). Solution phase sample analysis was carried out by attenuated total reflectance – Fourier transform infrared (ATR-FTIR, Thermo scientific, Nicolet iS5, USA) spectroscopy using a 2 μL drop of the reaction sample on the diamond sample holder to derive

the products. To understand the change in oxidation state of the metal ion and its influence in

CF_4 degradation process, ESR spectroscopy was performed with focused light of a 1000 W

high-pressure Hg lamp through an aqueous filter. The ESR spectra were measured at the X-

band (~9.7 GHz) and under liquid nitrogen conditions (77 K) with a Bruker EMX model

spectrometer.

3. Results and discussion

3.1 Generation of mediator.

Fig. 2A (curve a) shows the changes in ORP changes during the electrolysis of

mediator precursor containing $Cu^{2+}[Ni^{2+}(CN)_4]$ the electrolyzed solution. The ORP value of the

$Cu^{2+}[Ni^{2+}(CN)_4]$ electrolyzed solution was reached ~ − 500 mV from -50 mV after 4h

electrolysis could be Cu^{2+} to Cu^{1+} reduction. In order to crosscheck whether the Ni^{2+} reduction,

though the Ni^{1+} ORP value found -800 mV [21], occurred, the ORP value of only $[Ni^{2+}(CN)_4]^{2-}$

during electrolytic reduction was compared (Fig.2A curve b), where the ORP value reached

immediately to -700 mV indicating that Cu^{2+} is reduced instead of Ni^{2+} in the heterobimetallic

complex $(Cu^{2+}[Ni^{2+}(CN)_4])$. To confirm whether Cu^{2+} is reduced, the electrolyzed solution of

$Cu^{2+}[Ni^{2+}(CN)_4]$ was analyzed by ESR and the results are shown in Fig.2B. The ESR spectra

showed a typical pattern for the polycrystalline Cu^{2+} ion having near axial symmetry with g_{xx}

$\approx$ g_{yy} (~2.04) and g_{zz} (~2.26) and A_{xx} $\approx$ A_{yy} (~ 35 G) and A_{zz} (~190 G) values. The g values

and A_{xx}, A_{yy} and a large A_{zz} value, which is greater than 140 G confirmed the Cu^{2+} complex

with a square-planar geometry [27] (Fig.2B curve a). On the other hand, its reduced

monovalent Cu^{1+} species was ESR inactive. Therefore, at the same time, the electrolyzed

$Cu^{2+}[Ni^{2+}(CN)_4]$ samples showed a reduced intensity without a change in the symmetrical

values indicating Cu^{1+} formation with square planar geometry (Fig.2B curve b). Interestingly, the Cu^{1+} concentration was increased with increasing electrolysis time (Fig.3), which was derived by potentiometric titration. The Cu^{1+} concentration can be generated electrochemically a maximum of 3.1 mM in 5 h electrolysis time in the bimetallic complex $(Cu^{2+}[Ni^{2+}(CN)_4])$ under the given conditions.

3.2 CF_4 degradation by MER.

Once the Cu^{1+} concentration reached approximately 3 mM by electrolysis, the electrolyzed solution of $Cu^{1+}/Cu^{2+}[Ni^{2+}(CN)_4]$ was pumped into the scrubbing column through the top of the scrubbing column. Subsequently, 10 ppm of CF_4 was injected at 0.2 L min^{-1} into the bottom of the scrubbing column, while electrolysis was continued to regenerate the Cu^{1+}. Fig. 4 shows the results obtained under these conditions, where shows a decrease in Cu^{1+} concentration from 3.1 mM to 2.1 mM while inject 10 ppm of CF_4 into the scrubber that then decreases further to 1.2 mM in 1h CF_4 removal time. At the same time, there was almost 96% of feed CF_4 removed initially and keep maintained around 93% removal during studied time 1 h (inset figure). This explains CF_4 removal at room temperature by the electrogenerated $Cu^{1+}[Ni^{2+}(CN)_4]^{1-}$ is possible. This 96% CF_4 removal is not simply by absorption in to 10 M KOH solution because, CF_4 absorption into a 10 M KOH solution reached saturation in 5 min [21]. The Cu^{1+} concentration variation during the CF_4 removal process suggests that the CF_4 removal reaction follows the MER by electrogenerated $Cu^{1+}[Ni^{2+}(CN)_4]^{1-}$. The Cu^{1+} concentration started increased once the CF_4 feed stopped confirms the CF_4 removal sustainable by continuous generation of Cu^{1+} electrochemically.

Removal of CF_4 was undertaken at different gas flow rates (Fig. 5). At the lowest gas flow rate of 0.2 L min^{-1}, CF_4 removal was almost 100%. However, this decreased to 26% with

increasing gas flow rates to 2 L min^{-1}. This implies that the generation rate of Cu^{1+} is insufficient to sustain CF_4 removal as CF_4 loading is increased. Mass transfer analysis confirmed that above the flow rate of 0.2 L min^{-1}, a finite conversion rate of 13 to 18 µg CF_4 min^{-1} was achieved independent of gas flow rate (Figure 6 curve a). When the rate of mass transfer in gas-liquid systems is independent of gas velocity, the process can be described as liquid-phase controlled, which is characteristic of separations comprising solutes with limited solubility, such as CF_4 [28]. In this study, the reduction of CF_4 could have been within the liquid film or within the bulk, in which case CF_4 absorption would have been facilitated without electrogenerated mediator (Fig.1 in ref. 21). Liquid-phase resistance to mass transfer may therefore be enhanced through optimizing the ratio between the scrubber recycle rate (or gas-to-liquid ratio) and electrochemical recycle rate, to increase the rate of reaction, and obviate resistance imposed by the low solubility of the non-reduced primary solute. Feed concentration was increased from 10 ppm to 30 ppm CF_4, which reduced CF_4 removal efficiency from 95% to 30% (Fig.7). The time to steady-state increased to nearly 45 min at 30 ppm, which is ascribed to the sudden void of electrogenerated Cu^{1+} through reaction with the increased CF_4 injection. Mass transfer analysis demonstrated a consistent rate of reaction at steady-state, which indicates that CF_4 degradation was zero order with respect to concentration (Figure 6 curve b), such that the rate of separation from the gas phase will be dependent upon the concentration of free reactant Cu^{1+} in the liquid phase.

3.3 Product analysis.

The comparative in-situ gas FTIR spectra (Fig.8 curve e) confirms the formation of CH_3CH_2OH during the degradation of CF_4 by MER process, where the standard CF_4 and

CH_3CH_3OH were compared (Fig.8 curve a & b). At initial degradation process, there was observed no peak at CH_3CH_2OH frequency region (Fig.8 curve d) but CH_3CH_2OH peak found during its evolution timings (Fig.8 curve e) confirms the CH_3CH_2OH formation but, according to inset Fig.4, almost 96% CF_4 removal was achieved from the beginning of the removal process. Also, no products were observed at the scrubber in the first 30 min (Fig.SI 1curve a). After 30 min, a huge concentration of ethanol (CH_3CH_2OH) suddenly emerged at the scrubber exit at approximately 250 ppm (Fig.SI 1 curve a). In a similar time interval, trifluoroethane (CH_3CF_3) began to exit around 10 ppm (Fig.SI 1 curve b). Note that ethanol and HF were produced from the beginning of the removal process while the electrogenerated Co^{1+} mediator was used to remove CF_4 gas [21]. The CF_4 removal process followed mediated degradation to soluble products that exited after a saturation point was attained, which could explain the late exit of CH_3CH_2OH and CH_3CF_3. Surprisingly, no HF gas was coming out of the scrubber or exit gas (inset figure of Fig.SI 1) could be due to CH_3CF_3 intermediate formation by heterobimetallic complex ($Cu^{1+}[Ni^{2+}(CN)_4]^{1-}$). Noteworthy that in case of only electrogenerated mediator $[Ni^{1+}(CN)_4]^{3-}$, the CF_4 removal followed COF_2 intermediate pathway [21] to produce ethanol. Also, the CH_2CH_2OH formation found only at 0.2 L/min gas flow rate and **a**t higher gas flow rates 1 and 2 L min^{-1}, there found no CH_3CH_2OH peak but CH_3CF_3 peak appeared (Fig.SI 2 & 3) at its respective frequency region additionally support the CH_3CH_2OH formation only at low gas flow rate and also the reaction stopped at intermediate formation. The scrubbing solution underwent an ATR-FTIR analysis after the electro-scrubbing process was completed and reaction solution showed only CH_3CH_2OH present (-O-H and -C-O stretching frequencies well matched with the instrument library CH_3CH_2OH sample) in solution (Fig. SI 4), confirming that the reaction product is CH_3CH_2OH. Many electrochemical

reports have shown that CFCs form CH_4 and fluorine-reduced derivatives, such as CF_3CH, CH_2F_2, CH_3F, and CF_2CFCl [17-20] but, there are no reports on the formation of CH_3CH_2OH during the degradation of CF_4. Recently, direct ethanol formation was observed on a copper electrode during the reduction of CO_2 through carbon dioxide dimer formation [29,30]. Similarly, a carbon tetrafluoride dimer could have formed via the electrogenerated Cu^{1+}, which might have easily hydroxylated to ethanol, because the scrubbing solution is 10 M KOH, as shown by the proposed scheme 1. The possibility of dimerization was confirmed by the additional product CF_3CH_3 (Fig.8 curve b) found at the scrubber exit, which may be due to incomplete reaction or intermediate formation.

4. Conclusions

Electrogenerated $Cu^{1+}[Ni^{2+}(CN)_4]^{1-}$ successfully degraded CF_4 to ethanol without forming HF at room temperature. The electrogeneration of Cu^{1+} from the hetero-bimetallic complex of $Cu^{2+}[Ni^{2+}(CN)_4]$ was identified by ORP variation and confirmed the same by ESR spectroscopy analysis. The Cu^{1+} concentration variation during the injection of CF_4 into the scrubber column or the CF_4 removal process confirmed the degradation of CF_4 follows MER process. The online gas phase and offline solution phase FTIR analyses results confirmed that CH_3CH_2OH is a final product along with an intermediate or incomplete product CF_3CH_3 without corrosive product HF during the degradation of CF_4 using the electrogenerated $Cu^{1+}[Ni^{2+}(CN)_4]^{1-}$ in a highly KOH medium. Independent of mass transfer coefficient with feed CF_4 concentration confines the degradation follows zero order kinetics and chemical reaction controlled process, which enables to help scale-up the process.

ACKNOWLEDGEMENT

REFERENCES

[1]   A.R. Ravishankara, S. Solomon, A.A. Turnipseed, R.F. Warren, Science 259 (1993) 194-199.

[2]   W.-T. Tsai, H.-P. Chen, W.-Y. Hsien, J. Loss Prevent. Proc. 15 (2002) 65-75.

[3]   C. Rittmeyer, J. Vehlow, Chemosphere 26 (1993) 2129-2138.

[4]   C.W. Lee, J.V. Ryan, R.E. Hall, G.D. Kryder, B.R. Springsteen, Combust. Sci. Technol. 116-117 (1996) 455-478.

[5]   H.M. Lee, M.B. Chang, R.F. Lu, Ind. Eng. Chem. Res. 44 (2005) 5526-5534.

[6]   A. Gal, A. Ogata, S. Futamura, K. Mizuno, J. Phys. Chem. A 107 (2003) 8859-8866.

[7]   X.-F. Xu, J.Y. Jeon, M.H. Choi, H.Y. Kim, W.C. Choi, Y.-K. Park, J. Mol. Catal. A: Chem. 266 (2007) 131-138.

[8]   M.S. Gandhi, Y.S. Mok, J. Environ. Sci. (Beijing, China) 24 (2012) 1234-1239.

[9]   Narengerile, H. Saito, T. Watanabe, Plasma Chem. Plasma P. 30 (2010) 813-829.

[10]   H. Zhang, C.F. Ng, S.Y. Lai, Appl. Catal. B Environ. 55 (2005) 301-307.

[11]   X. Xu, X. Niu, J. Fan, Y. Wang, M. Feng, J. Nat. Gas Chem. 20 (2011) 543-546.

[12]   Y. Takita, M. Ninomiya, H. Miyake, H. Wakamatsu, Y. Yoshinaga, T. Ishihara, Phys. Chem. Chem. Phys. 1 (1999) 4501-4504.

[13]   M.M. Farris, A.A. Klinghoffer, J.A. RosSnl, D.E. Tevault, Catal. Today 11 (1992) 501-516.

[14]   N. Sonoyama, T. Sakata, Environ. Sci. Technol. 32 (1998) 375-378.

[15]   P.L. Cabot, L. Segarra, J. Casado, J. Electrochem. Soc. 151 (2004) B98-B104.

[16]   E.R. Wagoner, D.G. Peters, J. Electrochem. Soc. 160 (2013) G135-G141.

[17]   A. Schizodimou, G. Kyriacou, C. Lambrou, J. Electroanal. Chem. 471 (1999) 26-31.

[18] E.R. Wagoner, J.L. Hayes, J.A. Karty, D.G. Peters, J. Electroanal. Chem. 676 (2012) 6-12.

[19] P.L. Cabot, L. Segarra, J. Casado, Electrochem. Solid-State Lett. 6 (2003) B15-B18.

[20] R.E. Taylor-Smith, D. Sayres, Proc. - Electrochem. Soc. 99-8 (1999) 116-125.

[21] G. Muthuraman, I.S. Moon, J. Hazard. Mater. 325 (2017) 157-162.

[22] Z.M. El-Bahy, R. Ohnishi, M. Ichikawa, Appl. Catal., B Environ. 40 (2003) 81-91.

[23] Y. Takita, C. Morita, M. Ninomiya, H. Wakamatsu, H. Nishiguchi, T. Ishihara, Chem. Lett. (1999) 417-418.

[24] J.-Y. Song, S.-H. Chung, M.-S. Kim, M.-g. Seo, Y.-H. Lee, K.-Y. Lee, J.-S. Kim, J. Mol. Catal. A: Chem. 370 (2013) 50-55.

[25] A.M. Chippindale, S.J. Hibble, E. Marelli, E.J. Bilbe, A.C. Hannon, M. Zbiri, Dalton T. 44 (2015) 12502-12506.

[26] W.C. Fernelius, J.J. Burbage, N.E. Ballou, Potassium tetracyanonickelate(II), in: Inorganic syntheses, John Wiley & Sons, Inc., **2007**, pp. 227-228.

[27] M.G. Savelieff, T.D. Wilson, Y. Elias, M.J. Nilges, D.K. Garner, Y. Lu, P. Natl. Acad. Sci. USA 105 (2008) 7919-7924.

[28] P. Scharlin, R. Battino, J. Solution Chem. 21 (1992) 67-91.

[29] Y. Song, R. Peng, D.K. Hensley, P.V. Bonnesen, L. Liang, Z. Wu, H.M. Meyer, M. Chi, C. Ma, B.G. Sumpter, A.J. Rondinone, Chemistry Select 1 (2016) 6055-6061.

[30] K.P. Kuhl, E.R. Cave, D.N. Abram, T.F. Jaramillo, Energ. Environ. Sci. 5 (2012) 7050-7059.

Figure captions

Fig.1   Schematic experimental setup used to degrade CF_4 at wet-scrubber by electrochemically generated $Cu^{1+}[Ni^{2+}(CN)_4]^{1-}$

Fig.2   (A) Oxidation/reduction potential (ORP) variation during electrolysis of (a) 50 mM $Cu^{2+}[Ni^{2+}(CN)_4]$ and (b) 50 mM $[Ni^{2+}(CN)_4]^{2-}$ in 10 M KOH solution. Electrolysis conditions: Electrodes ($4\ cm^2$) = Pt (anode) and anodized Ti (cathode); Current density – 30 mA cm^{-2}; Solution flow rate = 70 ml min^{-1}.

(B) ESR spectra of frozen $Cu^{2+}[Ni^{2+}(CN)_4]$ in a 10 M KOH solution (a) before and (b) after electrolysis. The electrolysis conditions were the same as in legend of Fig.2A.

Fig.3   Formation efficiency of Cu^{1+} from $Cu^{2+}[Ni^{2+}(CN)_4]$ during electrolysis in 10 M KOH solution. The electrolysis conditions are the same as in the legend of Fig.2A..

Fig.4 Cu^{1+} concentration variation during MER of CF_4 gas at electro-scrubbing by scrubbing a solution of electrolyzed $Cu^{2+}/Cu^{1+}[Ni^{2+}(CN)_4]^{1-/0}$ solution. Inst figure shows CF_4 degradation efficiency variation with time. Conditions: Feed concentration of CF_4 = 10 ppm; Gas flow rate = 0.2 L min^{-1}; Scrubbing solution flow rate = 3 L min^{-1}. Solution flow rate to electrolytic cell = 2 L min^{-1}; Current density = 30 mAcm^{-2}; Electrodes area = 50 cm^2.

Fig.5   Effect of the gas flow rate (mentioned in the figure) with time on the removal of CF_4 using electrogenerated $Cu^{1+}[Ni^{2+}(CN)_4]^{1-}$ in a 10 M KOH solution at electro-scrubbing. The remaining experimental conditions are the same as in the legend of Fig.4.

Fig.6   Mass conversion rate with CF_4 feed concentration (a) and gas flow rate (b) during its degradation at electro-scrubbing by electrogenerated $Cu^{1+}[Ni^{2+}(CN)_4]^{1-}$ in 10 M KOH solution. The electrolysis and electroscrubbing experimental conditions are the same as

in the legend of Fig.4.

Fig.7 Effect of the CF_4 feed concentration variation with time on its removal by electrogenerated $Cu^{1+}[Ni^{2+}(CN)_4]^{1-}$ in 10 M KOH solution by electro-scrubbing. The remaining experimental conditions are the same as in the legend of Fig.4.

Fig.8 Real time FTIR spectra during the removal of CF_4 at different conditions for product CH_3CH_2OH identification: (a) Reference FTIR for CF_4; (b) Reference FTIR for CH_3CH_2OH; (c) During direct feed on CF_4; (d) During the MER of CF_4 at 30 min; (e) During the MER of CF_4 at 60 min. The remaining experimental conditions are the same as in the legend of Fig.4.

Figures

Fig.1
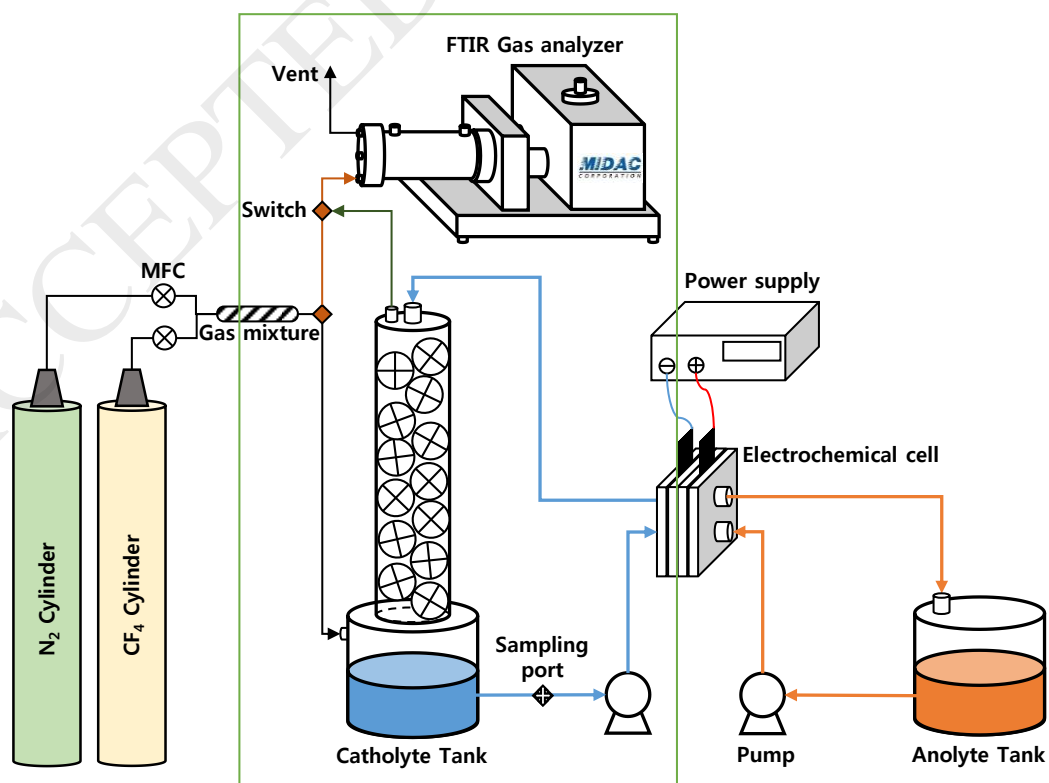
Fig.2
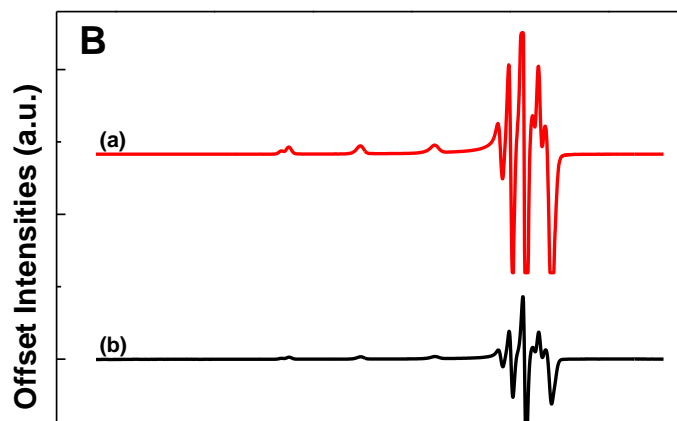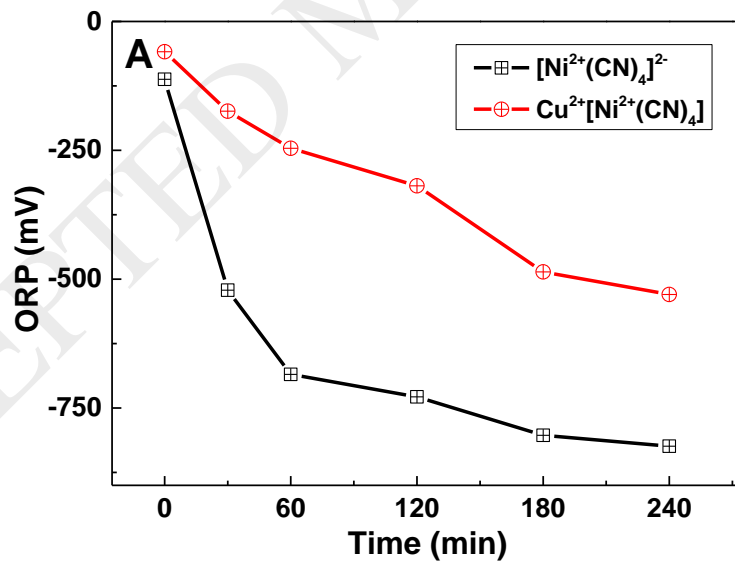
Fig.3

Fig.4

Fig.5

Fig.6

Fig.7

Fig.8

Figure axes: Absorbance (a.u.) vs Wave number (Cm^{-1})

(e)
(d)
(c)
Ref. CH$_3$CH$_2$OH
(b)
Ref. CF$_4$
(a)

Electrogenerated
$Cu^{1+}[Ni^{2+}(CN)_4]^{1-}$ $\qquad$ $Cu^{2+}[Ni^{2+}(CN)_4]$

CF_4 - - - - - - - - - - - - - - - -▶ CF_3CH_3 ──────▶ $CH_3CH_2OH + 2F_2$

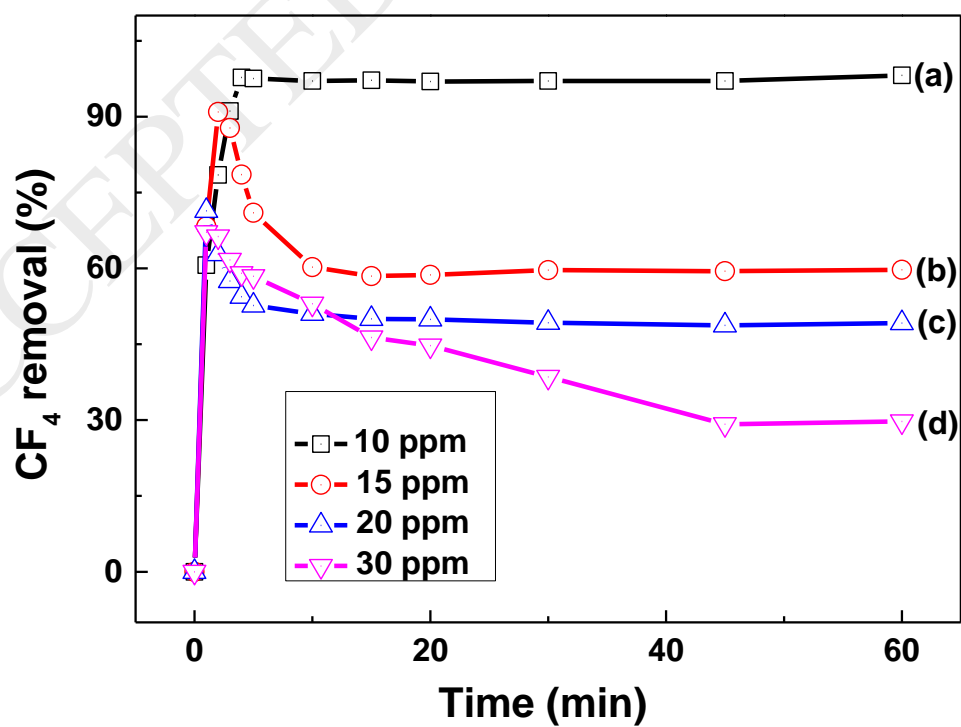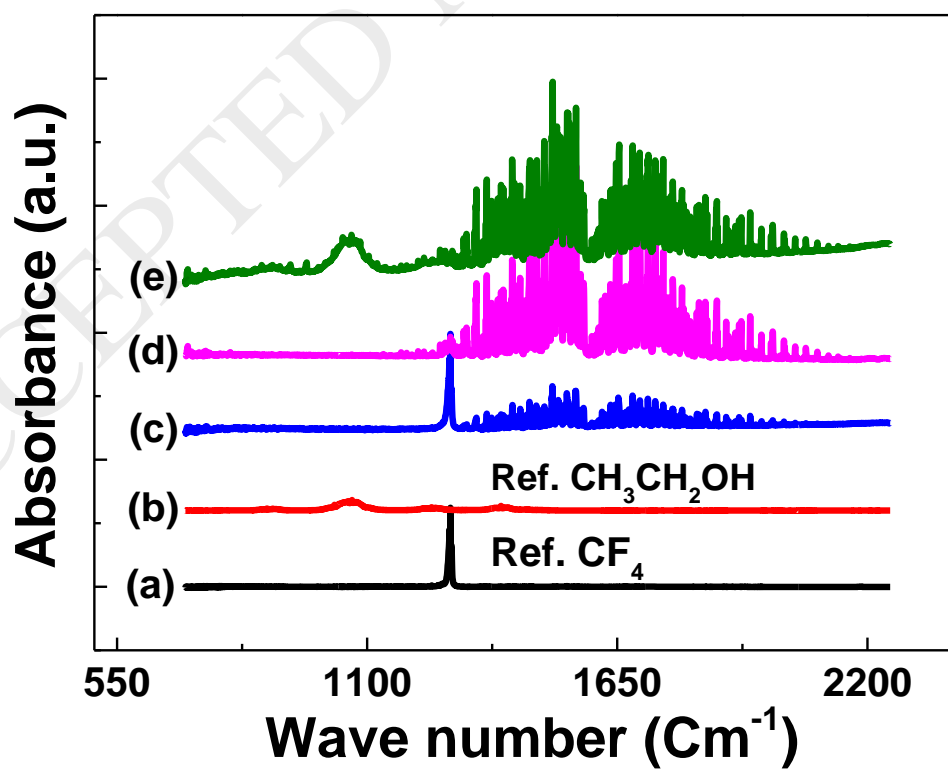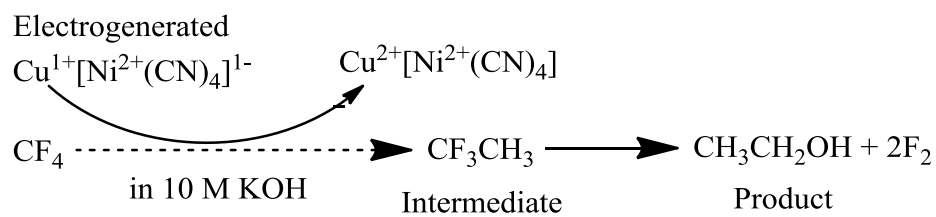$\qquad$ in 10 M KOH $\qquad$ Intermediate $\qquad$ Product
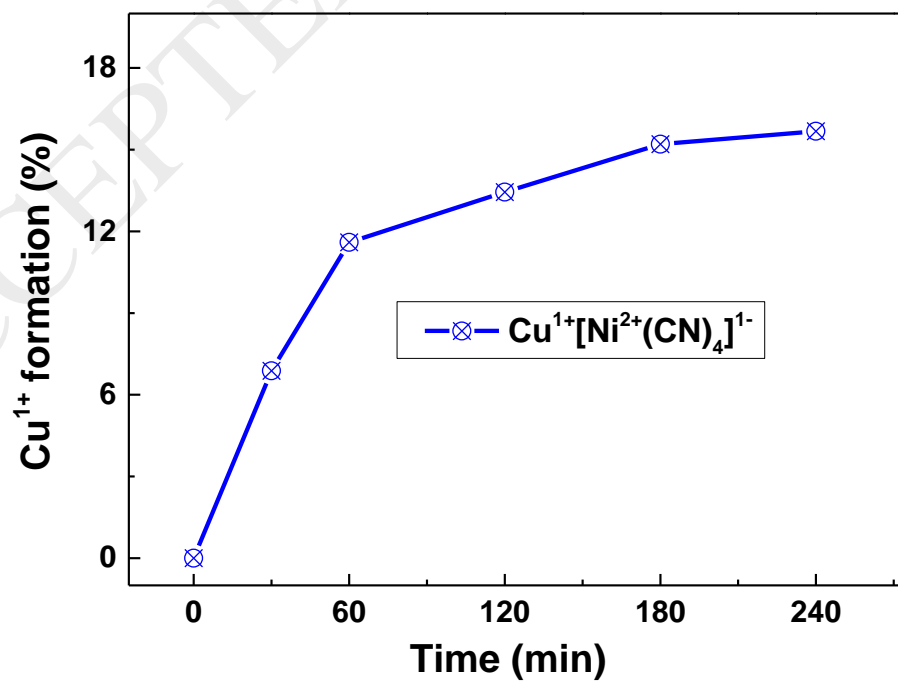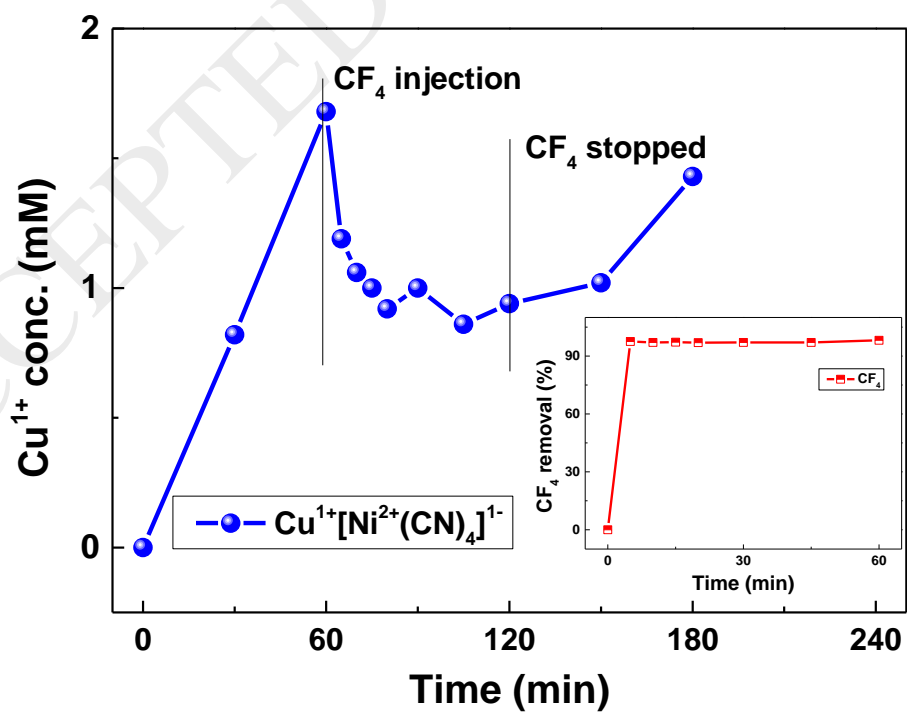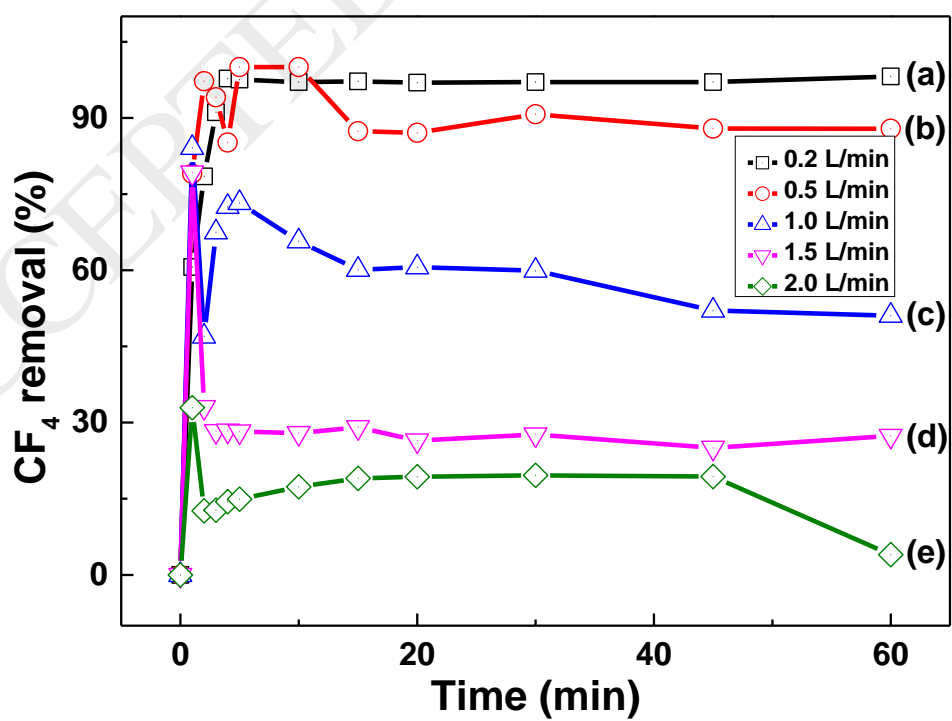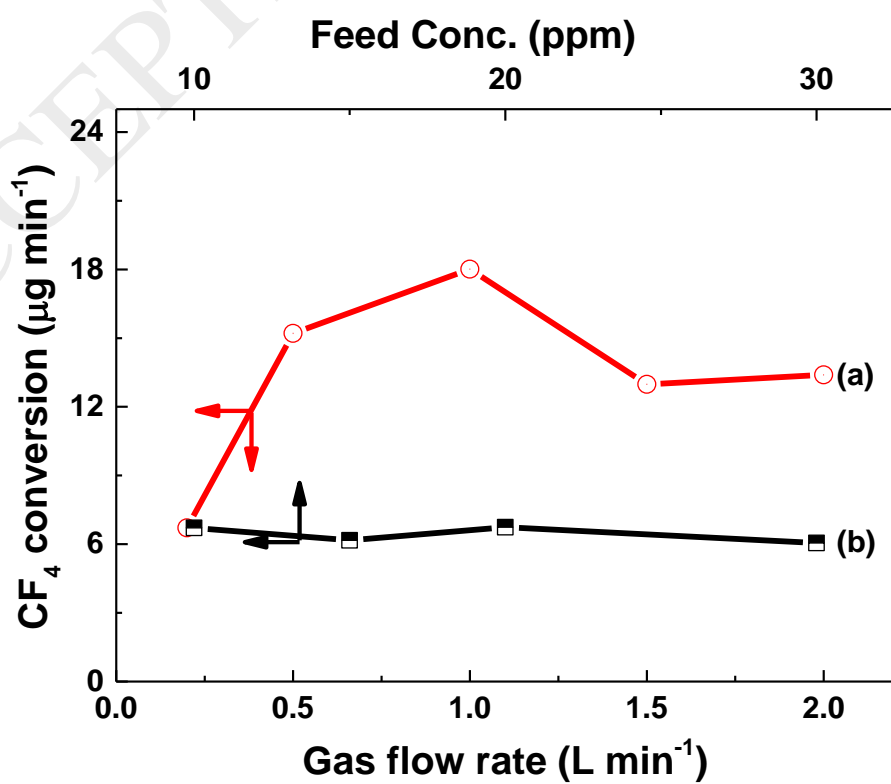
Scheme 1 $\qquad$ Plausible reaction pathway for CF_4 degradation to ethanol